PAPER 105 – ADSORPTION OF PHENOLS FROM TANNERY WASTEWATER USING MANGANESE DIOXIDE-ALBIZIA LEBBECK COMPOSITE

T. L. Adewoye [1], A. S. Atanda[1*], S. I. Mustapha[1], O. A. A. Eletta[1], A.A. Oguntuase[1], J.J. Kure[1], F.A. Aderibigbe[1], I. A. Mohammed[1]

[1]Department of Chemical Engineering, University of Ilorin, Ilorin, Nigeria.
[*]Email: sarat.morenikeji@gmail.com

ABSTRACT
This study investigated the removal of phenols from Tannery wastewater by batch adsorption process using MgO-modified adsorbent synthesized from *Albizia lebbeck* pods, which is an agricultural waste. Brunauer–Emmett-Teller (BET), scanning electron microscopy (SEM), energy dispersive X-ray spectrometry (EDS) and X-ray diffraction (XRD), characterized the unmodified Albizia lebbeck (ALC) and modified Albizia lebbeck (MAL) adsorbents synthesized. The BET surface area of the ALC and MALC were 221.5 and 255.8 m^2/g, respectively. The batch adsorption studies were conducted to investigate the effect of contact time, temperature and adsorbent dosage on the uptake of Phenol from tannery wastewater onto the adsorbents. The adsorbents showed maximum adsorption efficiencies of 79.01 and 81.21% for ALC and MALC respectively. The result from this study showed that the synthesized adsorbents were found to be effective for the treatment of tannery wastewater as the residual concentration of phenolic of the treated wastewater was very low and falls within permissible limits for effluent discharge.

KEYWORDS*:* Adsorption, Tannery wastewater, Manganese dioxide, *Albizia lebbeck*, Composite.

1. INTRODUCTION

Effluent from Industries and urbanization are major sources of water pollution in Nigeria, as process industries place little emphasis on wastewater management (UN-Water, 2011; Fouda *et al*; 2021). Industrial wastewater is disposed into water bodies partially treated or untreated posing a threat to environmental health and safety (Akpor & Muchie, 2011). Tanneries generate a large quantity of wastewater which contain chemicals, residual dyes, heavy metals, surfactants, salts, chlorinated substances, and so on low biodegradability (Oladipo *et al*., 2017;Fouda *et al*; 2021). Tannery wastewater is characterised by high salinity, high pH, heavy metals, high biochemical oxygen demand (BOD), chemical oxygen demand (COD) and phenol content as a result of organic materials in the hides and skins processed in this industry (Mohammed *et al*., 2013; Nayl *et al*., 2017; Costa & Olivi, 2009).

Phenol is a persistent organic compound formed from leather tanning process (Chaudry *et al*., 2022) which pose threat to environmental safety and water quality. Phenol and its derivatives accumulate in the fatty tissues of living organisms and exhibit highly toxic effects because they do not degrade easily. Phenol has multiple human health issues such as damage to DNA, weakening of muscles, necrotic lesions and burning in the mouth, stomach and oesophagus as well as pulse fluctuations (Bhattacharya *et al*., 2015; Chaudry *et al*., 2022). With the increasing population of Nigeria, the demand for clean water sources to engage for personal, agricultural and industrial use has risen considerably. A means of supplying this demand is to reduce pollution of natural water bodies, and improve wastewater management (UN-Water, 2018).

Researchers have used conventional methods for the treatment of wastewater (Ademiluyi, Amadi, & Amakama, 2009; Badalians Gholikandi, Baneshi, Dehghanifard, Salehi, & Yari, 2010; Mustapha *et al*., 2019). Adsorption is a very versatile process for treating industrial effluents out of all the methods. Easy-to-use, low-cost, and achievable with a wide number of materials of either mineral, organic or biological origins (Crini *et al*., 2018). Activated carbon in particular, has received tremendous attention as an adsorbent material due to its effectiveness in the adsorption of organic and inorganic pollutants from aqueous solutions. Activated carbon has a high surface area, a microporous structure, and a high degree of surface reactivity making it one of the most important industrial adsorbent materials (Bansal & Goyal, 2005). The high cost of activated carbon, however, poses the greatest obstacle to its widespread industrial use, as a treatment method must not only be effective, but must also be technologically and economically feasible (Crini *et al*., 2018).

Agricultural waste materials have received a considerable amount of attention as adsorbent materials as they are low-cost, easy to obtain, have low toxicity, and can be used to remove a variety of pollutants from industrial wastewater (Van *et al*., 2021). The complete replacement of conventional adsorbents by agricultural waste materials has, however, been impeded by the reduced specific adsorption capacities of these materials in their unmodified form compared to that of the conventional adsorbents (Do *et al*., 2019).

Manganese dioxide nanoparticles are one of several nanomaterials, which have attracted the interest of researchers for years due to their unique properties as adsorbents. The high surface area (Do *et al*., 2019) and high electrochemical activity (Zhou *et al*., 2012) of manganese dioxide nanoparticles makes them ideal as adsorbent materials. The incorporation of nanoparticles such as manganese dioxide with agricultural waste materials combines the adsorption capacities of both materials and creates a composite material with the individual characteristic of the two materials.

The objective of this study is therefore to produce a cheaper and effective adsorbent material from an agricultural waste material, *Albizia lebbeck,* and improve its performance by incorporating manganese dioxide nanoparticles.

2. THEORETICAL ANALYSIS

The reduction efficiencies of the synthesized adsorbent was determined using Equation (1).

$$\%removal = \frac{C_0 - C_e}{C_0} \times 100 \quad (1)$$

Where, C_0 and C_e (mg/l) are the concentration of phenol present in the tannery wastewater sample at the initial stage and equilibrium, respectively. The equilibrium amount (Q_e) of phenol removed per mass of adsorbent was evaluated using Equation 2.

$$Q_e = \frac{(C_0 - C_e)V}{W} \times 100 \quad (2)$$

Where, Q_e (mg/g) is the amount of phenol adsorbed per unit mass of adsorbent at equilibrium. V(l) is the volume of the solution and W(g) is the mass of the adsorbent used.

3. MATERIALS AND METHODS

3.1 Characterisation of Tannery Wastewater

The Physico-Chemical Properties of the tannery wastewater were investigated, determined and recorded using standard procedures by Nayl *et al*., (2017). The colour and smell of the wastewater were investigated by visual and olfactory examinations respectively. A pH meter was used to determine the pH and Turbidimeter was used determine turbidity. The Total Dissolved Solids (TDS) and the conductivity were estimated with a TDS meter and a conductivity meter, respectively. The COD and the BOD were determined using titrimetric methods. The dissolved oxygen analysis during the BOD test was performed using a dissolved oxygen meter. The phenol content of the wastewater was determined using a colorimetric method.

3.2 Phenol test

The phenol test was performed according to the procedure described by (Kupina et al., 2018). About 0.1 mL of the tannery water sample was measured into a test tube using a micropipette. About 0.5 mL and 0.4 mL of Folin C reagent was measured and 7.5% sodium carbonate was added sequentially to the test tube. The sample changed to a blue colour indicating the presence of phenol. The solution was allowed to stand for 30 minutes before being transferred into a cuvette. The cuvette was inserted into a spectrophotometer, and the absorbance of the solution was measured at 760 nm. The absorbance value obtained was converted to mg/L of phenol content using Equation 3:

$$y = 0.9787x \quad (3)$$

Where, y is the absorbance value measured and x is the concentration of phenol in mg/L

3.3 Preparation of leaf extract

The leaf extract was prepared according to the method used by Manik *et al.* (2020). Neem leaves were collected from the university of Ilorin premises and washed thoroughly with distilled water to remove all adhering impurities. The washed leaves was air-dried in a room away from direct sunlight. About 10 g of the cleaned leaves were placed into a 500 mL beaker containing 150 mL distilled water. The mixture was boiled at 90ºC for 20 minutes. The mixture was then cooled to room temperature and the neem leaf extract was obtained by filtering the mixture using a filter paper. The filtrate obtained was used without further modification for the synthesis

3.4 Synthesis of manganese dioxide nanoparticles

MgO nanoparticles were synthesized by hydrothermal method described by Ahmed *et al*., (2020) and Paul *et al*., (2017). About 50 mL of 0.2 M aqueous solution of potassium permanganate was prepared and mixed with 5mL of the leaf extract at 70ºC for 60 minutes with continuous stirring A brown ring was formed around the walls of the conical flask at the top of the $KMnO_4$ solution which indicates the formation of precipitate. The precipitate was then centrifuged at 3000 rpm for 15 min, and the synthesized nanoparticles were collected after the supernatant had been removed. The nanoparticles were then washed with distilled water three times to remove all impurities. The nanoparticles were dried in an oven at 100ºC for 10 h to evaporate all water (Adewoye *et al*., 2021).

3.5 Preparation of agricultural waste material

The *Albizia lebbeck* seed pods used in this study were collected from Mimosa trees located at the Faculty of Pharmaceutical Sciences in the University of Ilorin. The pods were emptied of all seeds, washed with clean water to remove all adhering dirt and other impurities, and then subsequently cleaned using a brush and distilled water. The washed pods were sun-dried for 7 days to reduce the moisture content and render them brittle enough for grinding. The dried *Albizia lebbeck* pods were ground into smaller fractions using a mortar and pestle. The ground pods were then further reduced in size using a blender. The obtained powder was sieved with 0.75µm to obtain particles of uniform size distribution. A portion of the sieved powder was calcined in a muffle furnace at 300ºC for three hours to produce the carbonized *Albizia lebbeck* pods (CAL).

3.6 Synthesis of manganese dioxide-Albizia lebbeck composite

The uncalcined *Albizia lebbeck pod powder* was modified with manganese dioxide nanoparticles via wet impregnation according to the process described by Aslam *et al*. (2019). About 5 g of the carbonizeded *Albizia lebbeck* (CAL) was dispersed in a 150 mL ethanol solution and shaken in a water bath shaker at 40ºC for 1 hour. About 1.5 g of the manganese dioxide nanoparticles were dispersed in another 150 mL ethanol solution and shaken in a water bath shaker at 40ºC for 1 hour. Afterwards, both ethanol solutions were mixed together and shaken in a water bath shaker at 40ºC for 1.5 hours to impregnate the powdered *Albizia lebbeck* with the manganese dioxide nanoparticles. The ethanol solution was evaporated by placing the beaker in an oven at 80ºC. The material obtained was then calcined in a muffle furnace at 300ºC to produce modified *Albizia lebbeck* composite adsorbent (MALC). Both the produced CAL and MALC were used for both batch adsorption studies without further modification

3.7 Characterization of the prepared adsorbent

The adsorbents prepared was characterised to determine it properties. The formation of the manganese dioxide nanoparticles was confirmed using UV-visible spectroscopy. The surface morphology of each adsorbent material was determined using scanning electron microscopy (SEM). The surface area of the composite adsorbent was determined using Brunauer-Emmet-Teller (BET) surface area analysis, the functional groups on the adsorbent were determined using Fourier Transform Infrared Spectroscopy (FTIR), and the size distribution of the adsorbent was determined using Dynamic Light Scattering (DLS) analysis (Chen *et al*., 2020).

3.8 Batch adsorption experiments

Batch adsorption experiments were carried out to determine the performance and adsorption isotherms of both adsorbents by treating a sample of tannery wastewater using phenolic content as a marker. The experiment was conducted using a 250 mL Erlenmeyer flask and a water bath shaker. The effects of contact time, temperature, and adsorbent dosage on the adsorption equilibrium were investigated. About 50 mL of the wastewater sample are filled into each of the flasks. The flasks were shaken with a sonnicator at a constant rate, allowing for sufficient mixing of the adsorbent and wastewater sample. For the effect of time experiments, the duration of shaking was varied between 10 to 90 minutes, at 20-minute intervals. The effect of temperature experiments was conducted over a range of temperatures from 30 to 55°C, with an interval of 5°C at the equilibrium time obtained from the previous experiment. The dosage of the adsorbent was varied between 0.2 to 1 g at 0.2 g intervals, at the equilibrium time and temperature obtained from the previous experiments, to determine the optimum dosage. The mixture obtained was filtered, the residual concentration of the phenol content was then analysed, and the reduction efficiencies were determined using Equation (2) .The equilibrium amount (Q_e) of phenol removed per mass of adsorbent was evaluated using equation 3.The adsorption isotherms of the adsorption of phenol unto each adsorbent were analyzed using Langmuir, Freundlich, and Temkins models. The kinetics of the adsorption experiment were determined using Pseudo first order, pseudo second order, and Elovic models.

4. RESULTS AND DISCUSSION

4.1 Characterization of tannery water

The tannery wastewater sample collected in this research is a non-viscous liquid with a large quantity of visible suspended solids and a very offensive odour. The initial colour of the wastewater on agitation is dirty purple due to the circulation of several grey suspended solids but turned to light pink when clarified. The presence of suspended solids in the wastewater may be attributed to the deposition of solid matter from the animal hide treated in the collected water sample, while the pink colour that appears on clarification of the wastewater may be ascribed to the presence of a similarly coloured dyestuff applied to the processing water for colouring the treated leather.

Prior to the adsorption experiment, the wastewater was analysed to determine its physico-chemical properties. The chemical properties of the wastewater were quantitatively analyzed and expressed as a function of its pH,

conductivity, turbidity, TDS, BOD, COD, TOC, and phenol content using standard procedures from literature. The results of the analyses and the standards set forth in the Federal Environmental Protection Agency Act of 1999 are presented in Table 1.

The pH of the wastewater at 8.33, and the COD value of the wastewater, determined to be 160 mg/L, both fall at the edge, but still within the permissible limit for effluent discharge for tanneries. The BOD of the wastewater sample is very low at 0.35, indicating a very low quantity of oxidizable organic material (Von Sperling, 2007). The total dissolved solids of the wastewater was also determined to be vastly above the permissible limit. The quantity of phenols found in the wastewater, measured to be 0.918 mg/L which is above the permissible limit for effluent discharge for tanneries, was selected as the environmental marker for the treatment procedure being an indicator of a high concentration of phenolic compounds in the wastewater. The high concentration of phenolic in the wastewater being a threat to human health and the safety of the environment.

All variations in the results of this analysis for tannery wastewater that differ from the values reported in literature may be due to local variation in manufacturing methods, processes, and processing chemicals used.

4.2 Manganese dioxide nanoparticles synthesis

The manganese dioxide nanoparticles produced via green synthesis as discussed in the previous section were analyzed to confirm their formation. Physical examination showed a brown, ultrafine solid material. The absorbance spectrum of a colloidal sample of the synthesized material was analyzed within a range of 200 – 800 nm using UV spectroscopy. The absorption spectra obtained is presented in Figure 1.

The synthesised material shows an absorbance peak value of 413 nm, implying that the synthesised material absorbs radiation in this spectrum. This is similar to the peak absorbance value reported in literature by Hoseinpour *et al*. (2018) for manganese dioxide nanoparticles. This indicates the formation of manganese dioxide nanoparticles.

4.3 Characterisation of adsorbents

The surface morphology of the prepared adsorbents was analyzed using SEM and the images obtained are presented in Fig. 1 (a) – (c).

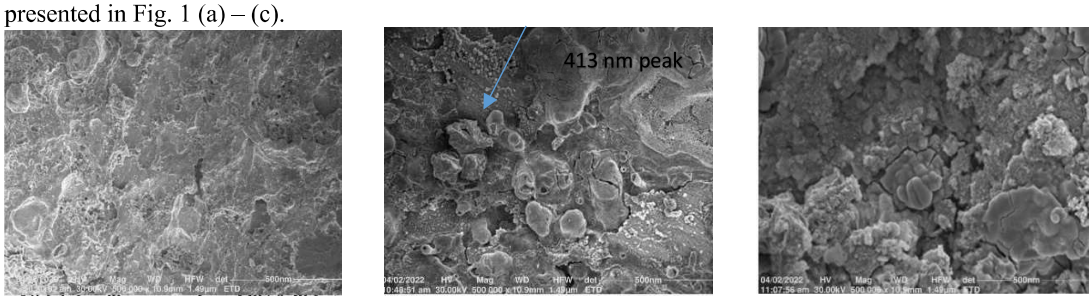

Fig. 1: SEM images for (a) manganese oxide nanoparticles (b) ALC adsorbent (c) MALC adsorbent

The images obtained from the SEM shows an enhanced image of the surface of each adsorbent. The manganese oxide nanoparticles show an almost unbroken surface as each particle is too small to be fully captured within the 500 nm range of the image. In the image for ALC and the composite, individual particles can be identified as the presence of the larger particles from the carbonized *Albizia lebbeck* are large enough to be seen individually. The surface image of ALC and MALC also bear a striking resemblance as the composite is modified from ALC.
The results obtained from the BET analysis are presented in Table 4.1.

Table 1: BET Analysis of the Prepared Adsorbents

Sample	Surface Area (m^2/g)	Pore Volume (cc/g)	Pore size (nm)
Manganese dioxide nanoparticles	127.8	0.04296	6.181
Carbonised *Albizia lebbeck* (ALC)	221.8	0.1011	6.929
Manganese dioxide-*Albizia lebbeck* composite (MALC)	255.1	0.08613	6.247

The result of the BET analysis showed a significant variation in the surface area of each adsorbent material. MALC is shown with the largest surface area, while the nanoparticle has the least. MALC is also observed to record a higher surface area than ALC, an increase that can be attributed to the additional surface area contributed by the nanomaterial added to ALC. These surface area values imply the availability of greater adsorption sites on MALC compared to ALC and the nanoparticle. Thus, in the absence of interference by functional groups on the surface of the composite, MALC was expected to perform better than ALC in an adsorption process.

There is also a variation in the pore size and pore volume of the adsorbent materials. The greatest pore volume and pore size recorded on ALC, with the lowest being recorded on the nanoparticle for both pore size and pore volume. MALC reported an intermediate value for pore size and pore volume, between the nanoparticle and ALC, which is as a result of the incorporation of the two materials. All three adsorbent materials are mesoporous, as the pore size of all three materials fall within the range of 2 – 50 nm (Zdravkov *et al*., 2007).

The results of the Dynamic Light Scattering analysis performed on each adsorbent material is recorded in Table 2.

Table 2: DLS analysis of the Prepared Adsorbents

Sample	Average hydrodynamic diameter (nm)
Manganese dioxide nanoparticles	Undefined (sample too polydispersed)
Carbonised *Albizia lebbeck* (ALC)	93.49
Manganese dioxide-*Albizia lebbeck* composite (MALC)	78.71

The DLS result revealed the average hydrodynamic diameter of each of the prepared adsorbents with the exception of the calcined manganese dioxide nanoparticles. The DLS analysis was unable to produce a definite average diameter for the nanoparticles as the sample was too polydispersed. This is one of the limitations of the DLS analysis, as a sample with widely varying size aggregates cannot be accurately measured through this technique (Tomaszewska *et al*., 2013). The dispersion of the manganese dioxide nanoparticles over a wide range of sizes is attributed to the aggregation tendency of manganese dioxide particles in solution. Individual particles clump together to form a larger particle. Thus, an additional technique may be required to accurately describe the size distribution of the manganese dioxide nanoparticles.

Both ALC and MALC report more favourable results in terms of the average hydrodynamic diameter, with both adsorbents showing a size distribution in the nanometre range. MALC reports the lower average diameter value of 78.71 nm, while ALC reports a slightly higher value of 93.49 nm. This is reasonable, as MALC is a composite of raw *Albizia lebbeck* and manganese dioxide nanoparticles. Thus, the lower average diameter may be attributed to the presence of the nanoparticles that was incorporated with the *Albizia lebbeck*.

4.4 Fourier Transform Infrared Spectroscopy (FTIR)

FTIR analysis revealed the functional groups present on each of the prepared materials. The results of the FTIR analysis performed on each adsorbent material is recorded in Figure A2. The FTIR spectra of the calcined manganese dioxide nanoparticle shows a broad absorption band between 3500 to 2500 cm^{-1}, with a peak at 3411.08 cm^{-1} which may be attributed to the stretching vibration of a hydroxyl group. The presence of the hydroxyl group is confirmed by the presence of a C-O group at 1052.24 cm^{-1}. The peaks appearing at the fingerprint region below 1500 cm^{-1} are compared to FTIR peaks obtained in the works of Hoseinpour *et al*. (2018) and Moon *et al*. (2015) to validate the appearance of an O-Mn-O bond. The peak at 526.65 cm^{-1} is related to the vibration of an O-Mn-O bond, the same bond reported by the two authors at 520 and 518 cm^{-1} respectively, indicating the formation of MnO_2 particles.

The calcined *Albizia lebbeck* displayed its first absorption peak at 3072.30 cm^{-1}, a region associated with a stretching C-H bond. The C-H bond is confirmed to be a C=C bond by the presence of weak absorption at 1,600 cm^{-1}. An absorption band at 2,211.08 cm^{-1} indicates the presence of a -C≡C- stretching bond. The presence of a C-O bond is observed by the presence of absorption at 1083.91, between 1000 to 1300 cm^{-1}. The sharp strong absorption band at 871.77 cm^{-1} is assigned to a C-H bending bond ($R_2C{=}CH_2$).

The absorption spectra of manganese dioxide-*Albizia lebbeck* composite displayed a similarity to the spectra of both the calcined manganese dioxide nanoparticle and to the calcined *Albizia lebbeck.* The first absorption band appeared at 3,411.08 cm^{-1}, a peak identical to that found on the nanoparticle spectra. This peak is assigned a stretching OH bond, whose presence is confirmed by the presence of a C-O bond at 1045.91 cm^{-1}. The presence of a -C≡C- stretching bond contributed by the *Albizia lebbeck* base is identified at 2195.25 cm^{-1}. A C=O stretching bond is attributed to a peak appearing at 1793.14 cm^{-1}, and the presence of a C-H bending bond caused by a methyl group is observed at 1460.69 cm^{-1}. The peak of the absorption band at 1045.91 cm^{-1} is attributed to the presence of a C-O bond, which could have been derived from the nanoparticles or the base compound. An absorption peak also exists at 878.10 cm^{-1}, a value similar to that on the *Albizia* lebbek spectra and denoting a C-H bending bond ($R_2C{=}CH_2$). The final significant peak appears at 507.65 cm^{-1}, a region close to the 526.65 cm^{-1} reported for the calcined manganese dioxide nanoparticles. This indicates the presence of an O-Mn-O bond in the modified material.

The work of Alabi *et al*. (2016) describes functional groups that facilitate the adsorption of phenols. This includes -$OH_{stretch}$ (hydroxyl), C=$C_{stretch}$ (aromatic), C-$H_{bending,}$ and C-$H_{strecth}$. Several of these are present on the materials analysed above, with the CAL adsorbent having three of the recognised groups with the exception of the -OH stretching bond.

4.5. Batch adsorption studies

4.5.1. Effect of contact time

The effect of contact time was investigated on the adsorption of phenol unto MALC and ALC in the range of 10 -90 min using 0.2 g of adsorbent in 50 mL of wastewater at 30°C as presented in Figure 2a. The removal efficiency of the both ALC and MALC increased with an increase in contact time. The removal efficiency of both adsorbents steadily increased until equilibrium was attained at 70 minutes, after which there was a sharp decrease in the removal efficiency. The decrease in removal efficiency observed in Figure 2b may be due to the filling of pores of adsorbents with water molecules (Parlayici *et al*., 2015). Hence, the retention time of 70 mins was chosen as the optimum time in this study. More so, the removal efficiency of MALC is obtained to be higher than that of ALC lower contact times, with ALC having the highest removal efficiency at equilibrium. It was also observed in adsorption studies that ALC dispersed in the wastewater remains on the surface before adsorption and it settle in the bottom of the flask after adsorption. This could be due to the increase in mass of the ALC particles due to the adsorption of phenol fact that the adsorbent is completely saturated and becomes heavier in weight.

4.5.2. Effect of temperature

Temperature has strong effect on the intermolecular force between the adsorbate and the adsorbent particles. Effect of temperature on the adsorption process was investigated and the result obtained are presented in Fig. 2b. An increase in the temperature causes a decrease in the efficiency of both ALC and MALC for phenol removal as shown in Fig. 2c. This inverse relationship indicated that the adsorption process is an exothermic process (Edet & Ifelebuegu, 2020). The decrease in adsorption capacity is due to the fact that at low temperatures, the kinetic energy of the particle is low and the intermolecular attractive forces are strong, hence, the molecules of the adsorbate are easily and strongly attracted to the surface of the adsorbent which gives a higher adsorption efficiency and vice versa.

4.5.3. Effect of dosage on the removal of phenol.

The effect of ALC and MALC dosage on the percentage reduction of phenol was studied at 45°C for 70 min. The adsorbent dosage was varied from 0.2 – 1.0g/100 ml as shown in Figure 2b. It was observed that the reduction efficiency increased with increasing adsorbent dose until the optimum dosage of 0.8 g/50 ml for MALC and 0.8 g/50 ml for MALC and ALC and corresponding to 79.01 and 81.21%, respectively. The highest phenol removal occurred at 0.8 g in both MALC and ALC. The removal efficiency of each adsorbent increases as the dosage increases. This increase in the removal efficiency may be due to the increase in the available functional groups and the total surface area of the adsorbents. Thus, more active sites are present for the adsorption of phenol from the wastewater. ALC has a higher removal percentage than the MALC.

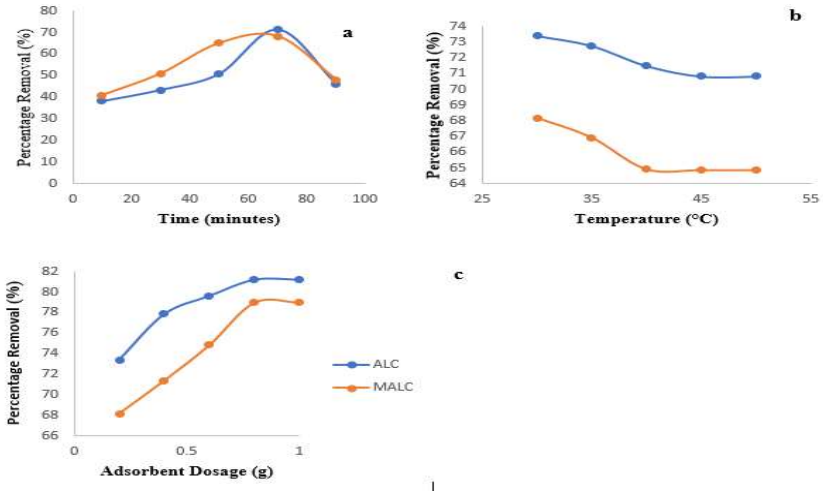

Fig. 2: Effect of (a) contact time, (b) temperature **(c)** dosage on the removal of phenol.

5. CONCLUSIONS

This study investigated the removal of phenol from Tannery wastewater by batch adsorption process using MgO-modified adsorbent synthesized from *Albizia lebbeck* pods, which is an agricultural waste. The un modified *Albizia lebbeck* (ALC) and modified *Albizia lebbeck* (MALC) adsorbent synthesized were characterized Brunauer–Emmett-Teller (BET), scanning electron microscopy (SEM), energy dispersive X-ray spectrometry (EDS) and X-ray diffraction (XRD). The BET surface area of the ALC and MALC were 221.5 and 255.8 m^2/g, respectively. The batch adsorption studies were conducted to investigate the effect of contact time, temperature and adsorbent dosage on the uptake of Phenol from tannery wastewater onto the adsorbents. The adsorbents showed maximum adsorption efficiencies of 79.01 and 81.21% for ALC and MALC respectively. The result from this study showed that the synthesized adsorbents were found to be effective for the treatment of tannery wastewater as the residual concentration of phenolic of the treated wastewater was very low and falls within permissible limits for effluent discharge.

ACKNOWLEDGEMENTS

We would like to express our gratitude to all those who have contributed to this research paper. Without your hardwork, expertise and dedication, this research would not have been possible.

REFERENCES

Achak, M., Elayadi, F., & Boumya, W. (2019). Chemical coagulation/flocculation processes for removal of phenolic compounds from olive mill wastewater: a comprehensive review. *Am. J. Appl. Sci*, *16*(3), 59-91.

Adewoye, T., Ogunleye, O., Abdulkareem, A., Salawudeen, T., & Tijani, J. (2021). Optimization of the adsorption of total organic carbon from produced water using functionalized multi-walled carbon nanotubes. *Heliyon*, *7*(1), e05866.

Ado, A., Tukur, A. I., Ladan, M., Gumel, S. M., Muhammad, A. A., Habibu, S., & Koki, I. B. (2015). A review on industrial effluents as major sources of water pollution in Nigeria. *Chemistry Journal*, *1*(5), 159-164.

Ahmed, M., Janyo, N., Sudi, I. Y., Gabriel, S., & Joh, I. (2020). Green Synthesis of Manganese Oxide Nanoparticles from Cassia ora Leaves and its Toxicological Evaluation. *Asian Journal of Applied Sciences*, *13*, 60-67. https://doi.org/10.3923/ajaps.2020.60.67

Akpor, O., & Muchie, B. (2011). Environmental and public health implications of wastewater quality. *African Journal of Biotechnology*, *10*(13), 2379-2387.

Al-Anber, M. A. (2011). *Thermodynamics approach in the adsorption of heavy metals*. IntechOpen.

Alabi, A. H., Buhari-Alade, A. I., Sholaru, F. O., & Awoyemi, R. F. (2016). Biosorption of phenols and dyes on Albizia lebbeck (Rattle seed) pod: equilibrium and kinetic studies. *International Journal of Environmental Sciences*, *5*(3), 154-165.

Alam, M. Z., Ahmad, S., & Malik, A. (2009). Genotoxic and mutagenic potential of agricultural soil irrigated with tannery effluents at Jajmau (Kanpur), India. *Archives of environmental contamination and toxicology*, *57*(3), 463-476.

Alam, M. Z., Ahmad, S., Malik, A., & Ahmad, M. (2010). Mutagenicity and genotoxicity of tannery effluents used for irrigation at Kanpur, India. *Ecotoxicology and Environmental Safety*, *73*(7), 1620-1628.

Ali Khan Rao, R., & Khatoon, A. (2017). Sorption studies for Cd (II) sequestration from aqueous solution on chemically modified Albizia lebbeck. *Separation Science and Technology*, *52*(3), 435-446.

Anku, W. W., Mamo, M. A., & Govender, P. P. (2017). Phenolic compounds in water: sources, reactivity, toxicity and treatment methods. *Phenolic compounds-natural sources, importance and applications*, 419-443.

Aslam, Z., Qaiser, M., Ali, R., Abbas, A., & Zarin, S. (2019). Al2O3/MnO2/CNTs nanocomposite: Synthesis, characterization and phenol adsorption. *Fullerenes, Nanotubes and Carbon Nanostructures*.

Awad, A. M., Jalab, R., Benamor, A., Nasser, M. S., Ba-Abbad, M. M., El-Naas, M., & Mohammad, A. W. (2020). Adsorption of organic pollutants by nanomaterial-based adsorbents: An overview. *Journal of molecular liquids*, *301*, 112335.

Ayub, S., Sharma, P. K., & Tripathi, C. N. (2014). Removal of hexavalent chromium using agro and horticultural wastes as low cost sorbents from tannery wastewater: A review. *International Journal of Research in Civil Engineering, Architecture & Design*, *2*(3), 21-35.

Bakar, A. F. A., & Halim, A. A. (2013). Treatment of automotive wastewater by coagulation-flocculation using poly-aluminum chloride (PAC), ferric chloride (FeCl 3) and aluminum sulfate (alum). AIP conference proceedings,

Bernard, E., Jimoh, A., & Odigure, J. (2013). Heavy metals removal from industrial wastewater by activated carbon prepared from coconut shell. *Res J Chem Sci*, *2231*, 606X.

Bhattacharya, A., Gupta, A., Kaur, A., & Malik, D. (2015). Simultaneous bioremediation of phenol and Cr (VI) from tannery wastewater using bacterial consortium. *International Journal of Applied Sciences and Biotechnology*, *3*(1), 50-55.

Bonilla-Petriciolet, A., Mendoza-Castillo, D. I., & Reynel-Ávila, H. E. (2017). *Adsorption processes for water treatment and purification*. Springer.

Chandra, R., Bharagava, R. N., Kapley, A., & Purohit, H. J. (2011). Bacterial diversity, organic pollutants and their metabolites in two aeration lagoons of common effluent treatment plant (CETP) during the degradation and detoxification of tannery wastewater. *Bioresource technology*, *102*(3), 2333-2341.

Chittoo, B. S., & Sutherland, C. (2020). Column breakthrough studies for the removal and recovery of phosphate by lime-iron sludge: Modeling and optimization using artificial neural network and adaptive neuro-fuzzy inference system. *Chinese Journal of Chemical Engineering*, *28*(7), 1847-1859.

Crini, G., Lichtfouse, E., Wilson, L. D., & Morin-Crini, N. (2018). Adsorption-oriented processes using conventional and non-conventional adsorbents for wastewater treatment. In *Green adsorbents for pollutant removal* (pp. 23-71). Springer.

Cueva-Orjuela, J. C., Hormaza-Anaguano, A., & Merino-Restrepo, A. (2017). Sugarcane bagasse and its potential use for the textile effluent treatment. *Dyna*, *84*(203), 291-297.

Do, Q. C., Choi, S., Kim, H., & Kang, S. (2019). Adsorption of lead and nickel on to expanded graphite decorated with manganese oxide nanoparticles. *Applied Sciences*, *9*(24), 5375.

Doble, M. (2007). Perry's chemical engineers' handbook. In: McGraw-Hill, New York, USA.

Durai, G., & Rajasimman, M. (2011). Biological treatment of tannery wastewater-a review. *Journal of Environmental science and Technology*, *4*(1), 1-17.

Ghosh, S., & Bandyopadhyay, A. (2017). Adsorption of methylene blue onto citric acid treated carbonized bamboo leaves powder: Equilibrium, kinetics, thermodynamics analyses. *Journal of molecular liquids*, *248*, 413-424.

Hadi, S. M., Al-Mashhadani, M. K., & Eisa, M. Y. (2019). Optimization of dye adsorption process for Albizia lebbeck pods as a biomass using central composite rotatable design model. *Chemical Industry and Chemical Engineering Quarterly*, *25*(1), 39-46.

Hoseinpour, V., Souri, M., & Ghaemi, N. (2018). Green synthesis, characterisation, and photocatalytic activity of manganese dioxide nanoparticles. *Micro & Nano Letters*, *13*(11), 1560-1563.

Jiang, J.-Q. (2015). The role of coagulation in water treatment. *Current Opinion in Chemical Engineering*, *8*, 36-44.

Joshi, N. C., Joshi, E., & Singh, A. (2020). Biological synthesis, characterisations and antimicrobial activities of manganese dioxide (MnO2) nanoparticles. *Research Journal of Pharmacy and Technology*, *13*(1), 135-140.

Karunarathne, H., & Amarasinghe, B. (2013). Fixed bed adsorption column studies for the removal of aqueous phenol from activated carbon prepared from sugarcane bagasse. *Energy Procedia*, *34*, 83-90.

Kupina, S., Fields, C., Roman, M. C., & Brunelle, S. L. (2018). Determination of total phenolic content using the Folin-C assay: Single-laboratory validation, First action 2017.13. *Journal of AOAC International*, *101*(5), 1466-1472.

Liu, C., Ding, R., & Xie, F. (2020). Facile synthesis of manganese dioxide nanoparticles for efficient removal of aqueous As (III). *Journal of Chemical & Engineering Data*, *65*(8), 3988-3997.

Luu, T. L., Tien, T. T., Duong, N. B., & Phuong, N. T. T. (2020). Tannery wastewater treatment after biological pretreatment by using electrochemical oxidation. In *Frontiers in Water-Energy-Nexus—Nature-Based Solutions, Advanced Technologies and Best Practices for Environmental Sustainability* (pp. 161-163). Springer.

Manasa, R. L., & Mehta, A. (2020). Wastewater: Sources of Pollutants and Its Remediation. *Environmental Biotechnology*, *2*, 197-219.

Manik, U., Nande, A., Raut, S., & Dhoble, S. (2020). Green synthesis of silver nanoparticles using plant leaf extraction of Artocarpus heterophylus and Azadirachta indica. *Results in Materials*, *6*, 100086.

Mariod, A. A., Saeed Mirghani, M. E., & Hussein, I. (2017). Chapter 41 - Albizia lebbeck (L. Benth.) Lebbeck Tree Seed. In A. A. Mariod, M. E. Saeed Mirghani, & I. Hussein (Eds.), *Unconventional Oilseeds and Oil Sources* (pp. 277-281). Academic Press. https://doi.org/https://doi.org/10.1016/B978-0-12-809435-8.00041-X

Masoud, M. S., El-Saraf, W. M., Abdel-Halim, A. M., Ali, A. E., Mohamed, E. A., & Hasan, H. M. (2016). Rice husk and activated carbon for waste water treatment of El-Mex Bay, Alexandria Coast, Egypt. *Arabian Journal of Chemistry*, *9*, S1590-S1596.

Mohammed, H., Hamza, A., Adamu, I., Ejila, A., Waziri, S., & Mustapha, S. (2013). BOD5 removal from tannery wastewater over ZnO-ZnFe2O4 composite photocatalyst supported on activated carbon. *Journal of Chemical Engineering and Materials Science*, *4*(6), 80-86.

Moon, S. A., Salunke, B. K., Alkotaini, B., Sathiyamoorthi, E., & Kim, B. S. (2015). Biological synthesis of manganese dioxide nanoparticles by Kalopanax pictus plant extract. *IET nanobiotechnology*, *9*(4), 220-225.

Mustapha, S., Shuaib, D., Ndamitso, M., Etsuyankpa, M., Sumaila, A., Mohammed, U., & Nasirudeen, M. (2019). Adsorption isotherm, kinetic and thermodynamic studies for the removal of Pb (II), Cd (II), Zn (II) and Cu (II) ions from aqueous solutions using Albizia lebbeck pods. *Applied water science*, *9*(6), 1-11.

Nayl, A. E. A., Elkhashab, R. A., Malah, T. E., Yakout, S. M., El-Khateeb, M. A., Ali, M. M. S., & Ali, H. M. (2017). Adsorption studies on the removal of COD and BOD from treated sewage using activated carbon prepared from date palm waste. *Environment Science Pollution Resources*, 1-10.

Okereke, J., Ogidi, O., & Obasi, K. (2016). Environmental and health impact of industrial wastewater effluents in Nigeria-A Review. *International Journal of Advanced Research in Biological Sciences*, *3*(6), 55-67.

Oladipo, A. A., Adeleye, O. J., Oladipo, A. S., & Aleshinloye, A. O. (2017). Bio-derived MgO nanopowders for BOD and COD reduction from tannery wastewater. *Journal of water process engineering*, *16*, 142-148.

Oubagaranadin, J. U. K., & Murthy, Z. (2011). Activated carbons: Classifications, properties and applications. *Activated Carbon: Classifications, Properties and Applications. Nova Science Publishers Inc, USA*, 239-266.

Patel, H. (2019). Fixed-bed column adsorption study: a comprehensive review. *Applied water science*, *9*(3), 1-17.

Ranade, V. V., & Bhandari, V. M. (2014). *Industrial wastewater treatment, recycling and reuse*. Butterworth-Heinemann.

Rocha, P. D., Franca, A. S., & Oliveira, L. S. (2015). Batch and column studies of phenol adsorption by an activated carbon based on acid treatment of corn cobs. *International Journal of Engineering and Technology*, *7*(6), 459.

Samarghandi, M. R., Al-Musawi, T. J., Mohseni-Bandpi, A., & Zarrabi, M. (2015). Adsorption of cephalexin from aqueous solution using natural zeolite and zeolite coated with manganese oxide nanoparticles. *Journal of molecular liquids*, *211*, 431-441.

Saxena, G., Chandra, R., & Bharagava, R. N. (2016). Environmental pollution, toxicity profile and treatment approaches for tannery wastewater and its chemical pollutants. *Reviews of Environmental Contamination and Toxicology Volume 240*, 31-69.

Sonune, A., & Ghate, R. (2004). Developments in wastewater treatment methods. *Desalination*, *167*, 55-63.

Tatah, V., Ibrahim, K., Ezeonu, C., & Otitoju, O. (2017). Biosorption kinetics of heavy metals from fertilizer industrial waste water using groundnut husk powder as an adsorbent. *J Appl Biotechnol Bioeng*, *2*(6), 221-228.

Tien, C. (2018). *Introduction to adsorption: Basics, analysis, and applications*. Elsevier.

Tomaszewska, E., Soliwoda, K., Kadziola, K., Tkacz-Szczesna, B., Celichowski, G., Cichomski, M., Szmaja, W., & Grobelny, J. (2013). Detection limits of DLS and UV-Vis spectroscopy in characterization of polydisperse nanoparticles colloids. *Journal of Nanomaterials*, *2013*.

UN-Water. (2011). *Policy brief: water quality* (United Nations. Available online at: http://www. unwater. org/downloads/waterquality_policybrief. pdf, Issue.

UN-Water. (2018). *Water Quality and Wastewater* (United Nations. Available online at: https://www.unwater.org/app/uploads/2018/10/, Issue.

Van, H. T., Nguyen, L. H., Dang, N., Chao, H.-P., Nguyen, Q. T., Nguyen, T. H., Nguyen, T. B. L., Van Thanh, D., Nguyen, H. D., & Thang, P. Q. (2021). The enhancement of reactive red 24 adsorption from aqueous solution using agricultural waste-derived biochar modified with ZnO nanoparticles. *RSC Advances*, *11*(10), 5801-5814.

Von Sperling, M. (2007). *Wastewater characteristics, treatment and disposal*. IWA publishing.

Worch, E. (2021). *Adsorption technology in water treatment*. de Gruyter.

Yi, Q. (2009). *Point Sources of Pollution: Local Effects and their Control-Volume II*. EOLSS Publications.

Zdravkov, B., Čermák, J., Šefara, M., & Janků, J. (2007). Pore classification in the characterization of porous materials: A perspective. *Open Chemistry*, *5*(2), 385-395.

Zekić, E., Vuković, Ž., & Halkijević, I. (2018). Application of nanotechnology in wastewater treatment. *Građevinar*, *70*(04.), 315-323.

Zhou, D., Liu, Q., Cheng, Q., Zhao, Y., Cui, Y., Wang, T., & Han, B. (2012). Graphene-manganese oxide hybrid porous material and its application in carbon dioxide adsorption. *Chinese science bulletin*, *57*(23), 3059-3064.

Edet, U. A., & Ifelebuegu, A. O. (2020). Kinetics, isotherms, and thermodynamic modeling of the adsorption of phosphates from model wastewater using recycled brick waste. *Processes, 8*(6), 665.

APPENDICES

Table A1: Comparison of the results of wastewater characterisation with set standards by FEPA

Parameters	Sample analysis values	Permissible limit (FEPA)
pH	8.33	6 – 9
Conductivity (mS/cm)	1.425	-
Turbidity (NTU)	3.808	-
TDS (mg/L)	715	30
TOC (%)	1	-
COD (mg/L)	160	164
BOD (mg/L)	0.35	50
Phenolics (mg/L)	0.918	0.2
Pb	1.132	-
Cd	1.002	-
As	0.487	-
Cr	1.477	-
Mn	0.252	-
Fe	0.864	-
Cu	0.132	-
Zn	0.434	-

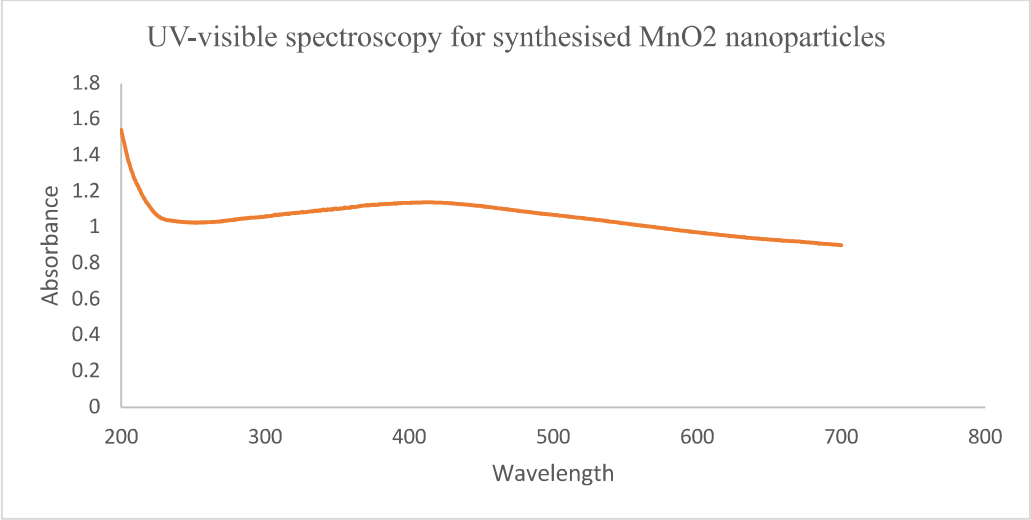

Fig. A1: UV-visible Spectroscopy for Synthesized MnO_2 Nanoparticles

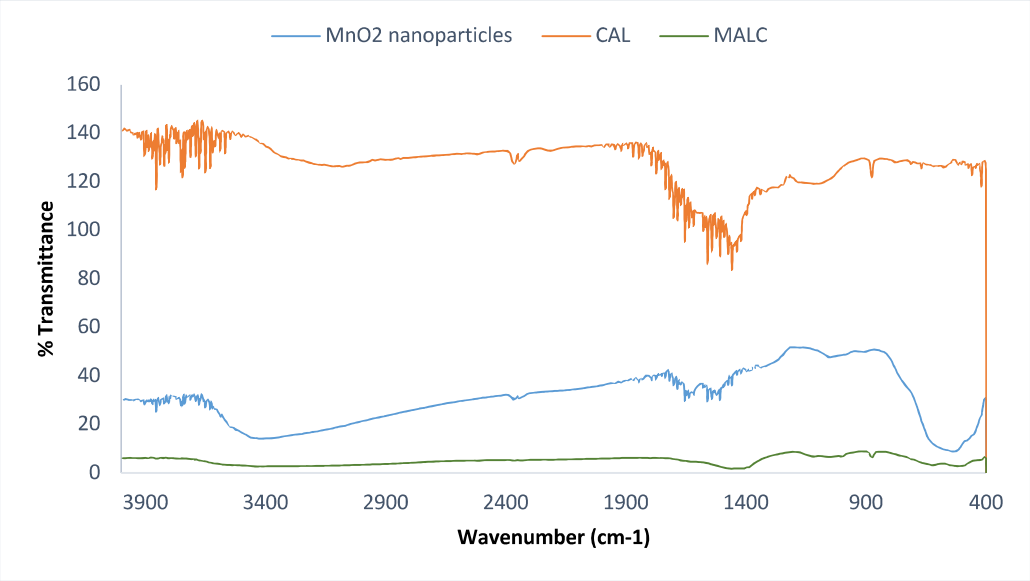

Figure A2: FTIR analysis of the MnO_2 nanoparticles, ALC and MALC